

Single atom laser in normal-superconductor quantum dots

Gianluca Rastelli^{1,2} and Michele Governale³

¹*Fachbereich Physik, Universität Konstanz, D-78457 Konstanz, Germany*

²*Zukunftskolleg, Universität Konstanz, D-78457 Konstanz, Germany*

³*School of Chemical and Physical Sciences and MacDiarmid Institute for Advanced Materials and Nanotechnology, Victoria University of Wellington, P.O. Box 600, Wellington 6140, New Zealand*



(Received 28 April 2019; revised manuscript received 14 August 2019; published 28 August 2019)

We study a single-level quantum dot strongly coupled to a superconducting lead and tunnel coupled to a normal electrode which can exchange energy with a single-mode resonator. We show that such a system implements a single atom laser. We employ both a semiclassical treatment and a quantum master-equation approach to characterize the properties of this laser. In particular, we find that this system can be operated with efficiency approaching unity; that is, a single photon is emitted into the cavity for every Cooper pair participating in the charge current. We find also that lasing in the proposed setup is clearly identifiable in the transport properties: in the lasing state, the electrical current through the quantum dot is pinned to the maximum value achievable in this hybrid nanostructure, and hence, the onset of lasing can be detected simply by a current measurement.

DOI: [10.1103/PhysRevB.100.085435](https://doi.org/10.1103/PhysRevB.100.085435)

I. INTRODUCTION

Hybrid nanoscale systems combine elemental components of different natures and provide a way to explore novel mechanisms of coherent energy exchange. Hybrid nanoscale systems that are commonly studied experimentally include quantum dots coupled to localized harmonic oscillators such as microwave photon cavities [1–6] and mechanical resonators [7–11]. In particular, these systems can realize single atom lasers [12,13]. Besides photon cavities, nanomechanical systems can also sustain *phonon* lasing, for instance, in a superconducting single-electron-transistor setup [14]. Single atom lasers exhibit unique features compared to conventional lasers, such as multistability [12,14–18]. Furthermore, such hybrid nanoscale systems are ideal platforms to explore correlations between charge transport and nonequilibrium photon states [19–26]. Early theoretical studies proposed lasing in a double-dot system on the basis of pure inelastic electron tunneling with single-photon emission [27–29]. However, single atom lasing has been achieved experimentally in double-dot systems [30,31] only in the phonon-assisted gain regime, where electron tunneling events are enhanced via simultaneous emission of a phonon besides the photon pumped into the cavity [32,33].

In this paper we demonstrate that single atom lasing can be achieved in a quantum dot with a single orbital level, strongly coupled to a superconducting lead. In Figs. 1(a) and 1(b) we show a specific example with a microwave photon cavity, similar to the experimental setup of Ref. [3]. Such a lasing system has an extremely appealing feature: it can be operated in a regime in which a single photon is emitted into the cavity almost for each Cooper pair participating in the charge current (efficiency $\beta \approx 1$). This high pumping efficiency is related to another interesting result: in the lasing state, the current is pinned to the maximum value that characterizes the system in the large-gap limit.

Before discussing our results in detail, we wish to give an intuitive description of how lasing occurs in this system. In the limit of a large superconducting gap, Andreev bound states, $|+\rangle$ and $|-\rangle$, are formed in the dot. These are coherent superpositions of the empty and doubly occupied dot states, $|0\rangle$ and $|D\rangle$, respectively. At high bias voltage, the normal lead behaves as a source of electrons; hence, only the empty state $|0\rangle$ can transition by tunneling to one of the singly occupied states $|\sigma\rangle$, which in turn can transition to the doubly occupied state $|D\rangle$ [Fig. 1(c)]. At sufficiently large energy detuning δ , between states $|D\rangle$ and $|0\rangle$, state $|-\rangle$ has a larger component of state $|0\rangle$, whereas $|+\rangle$ is mostly state $|D\rangle$. This implies that the transitions $|-\rangle \rightarrow |\sigma\rangle$ and $|\sigma\rangle \rightarrow |+\rangle$ are favored over the opposite transitions [Fig. 1(d)]. This symmetry breaking is ultimately the reason for lasing. Additionally, the product states corresponding to different occupations of the resonator (Fock states) and the Andreev bound states, $|\pm, n\rangle \equiv |\pm\rangle \otimes |n\rangle$, are mixed by the interaction between the charge on the dot and the resonator mode [curved dashed arrows in Fig. 1(e)]. As explained above, for the right choice of system parameters (detuning δ), tunneling with the normal lead favors the chain of transitions $|-, n\rangle \rightarrow |\sigma, n\rangle \rightarrow |+, n\rangle$, in which the state of the resonator is not modified. The interaction with the resonator then brings $|+, n\rangle$ into $|-, n+1\rangle$, and the process can start again. This leads to an increasingly higher occupation of the resonator mode [Fig. 1(e)]. Eventually, this energy-pumping mechanism is balanced by the intrinsic losses of the resonator, and hence, a steady state with a large but finite average occupation \bar{n} is established. More precisely, we show that the resonator reaches a lasing state in the steady-state regime. In particular, by tuning the orbital energy level of the dot ε_0 , one can control the energy splitting $2\epsilon_A$ between states $|+\rangle$ and $|-\rangle$. Accordingly, one can achieve the resonant condition for the coupling between the dot's degree of freedom and the resonator mode when $2\epsilon_A = \hbar\omega_0$, with ω_0 being the resonator's frequency.

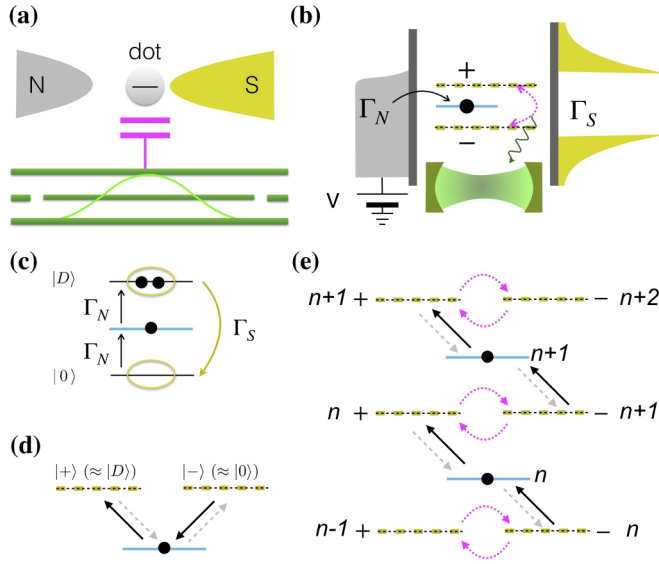


FIG. 1. (a) Device setup: a quantum dot between a superconductor (S) and a normal metal (N) is capacitively coupled to a microwave cavity. (b) In the rotating-wave approximation, the states $|+\rangle$ and $|-\rangle$ indicated by the yellow dashed lines are dynamically coupled to the resonator. The blue solid line denotes the singly occupied states $|\sigma\rangle$. Γ_N/\hbar is the tunneling rate from N, and Γ_S is the effective pairing potential in the quantum dot. (c) In the high-bias voltage limit, only the empty state $|0\rangle$ can transition to the singly occupied state, which in turn can transition to the doubly occupied state $|D\rangle$. (d) At positive and large detuning δ , the states $|+\rangle \approx |D\rangle - \frac{\Gamma_S}{2\delta}|0\rangle$ and $|-\rangle \approx |0\rangle + \frac{\Gamma_S}{2\delta}|D\rangle$. This breaks the symmetry in the transitions between the states $|\pm\rangle$ and $|\sigma\rangle$. (e) Schematic description of the pumping mechanism using the level diagram of the quantum dot coupled to the resonator.

This paper is organized as follows. In Sec. II we present the model of the system. In Sec. III, starting from a Lindblad equation in the rotating-wave approximation (RWA), we develop a semiclassical theory to estimate the value of the lasing threshold for the coupling strength between the dot and the resonator [34]. In Sec. IV, we supplement the semiclassical treatment by a quantum master-equation approach in order to evaluate the effect of quantum fluctuations. Results are discussed in Sec. V. Finally, conclusions are briefly drawn in Sec. VI.

II. MODEL

The Hamiltonian of the system can be written as $H = H_{\text{osc}} + H_{\text{int}} + H_{\text{dS}} + H_{\text{tun}} + H_N$. The quantum dot coupled to the superconductor in the large-gap limit is described by the effective Hamiltonian [35]

$$H_{\text{dS}} = \varepsilon_0 \sum_{\sigma=\uparrow,\downarrow} n_{\sigma} + U n_{\uparrow} n_{\downarrow} - \frac{\Gamma_S}{2} (d_{\uparrow}^{\dagger} d_{\downarrow}^{\dagger} + d_{\downarrow} d_{\uparrow}), \quad (1)$$

where d_{σ} (d_{σ}^{\dagger}) is the annihilation (creation) operator for an electron with spin $\sigma = \uparrow, \downarrow$ and $n_{\sigma} = d_{\sigma}^{\dagger} d_{\sigma}$. The Hilbert space of the dot is spanned by the states $|0\rangle$ (empty), $|\sigma\rangle = d_{\sigma}^{\dagger}|0\rangle$ (singly occupied with spin σ), and $|D\rangle = d_{\uparrow}^{\dagger} d_{\downarrow}^{\dagger}|0\rangle$ (doubly occupied). The detuning between the energy of the doubly occupied state and the empty state, $\delta = 2\varepsilon_0 + U$, determines

the strength of the proximity effect in the dot. The eigenstates of the effective Hamiltonian are the singly occupied states $|\sigma\rangle$ with eigenenergies $E_{\sigma} = \varepsilon_0$ and the states $|\pm\rangle$, which are coherent superpositions of $|D\rangle$ and $|0\rangle$ and read

$$|+\rangle = \cos(\theta)|D\rangle - \sin(\theta)|0\rangle, \quad (2a)$$

$$|-\rangle = \sin(\theta)|D\rangle + \cos(\theta)|0\rangle, \quad (2b)$$

with energies $E_{\pm} = \delta/2 \pm \varepsilon_A$ and coefficients $\cos(\theta) = (1/\sqrt{2})[1 + \delta/(2\varepsilon_A)]^{1/2}$ and $\sin(\theta) = (1/\sqrt{2})[1 - \delta/(2\varepsilon_A)]^{1/2}$. The energy $2\varepsilon_A = \sqrt{\delta^2 + \Gamma_S^2}$ is the splitting between the $|+\rangle$ and the $|-\rangle$ states. The normal lead is described by $H_N = \sum_{k\sigma} (\varepsilon_k - \mu_N) c_{k\sigma}^{\dagger} c_{k\sigma}$, with the lead-electron operators $c_{k\sigma}$ and $c_{k\sigma}^{\dagger}$. We choose as the energy reference the chemical potential of the superconductor μ_S and set, without loss of generality, $\mu_S = 0$. The chemical potential of the normal lead is $\mu_N = eV$, where e is the electron charge and V is the voltage difference between the normal lead and the superconductor. The tunneling between the lead and the dot is modeled by the tunneling Hamiltonian $H_{\text{tun}} = V \sum_{k\sigma} c_{k\sigma}^{\dagger} d_{\sigma} + \text{H.c.}$ We assume that the density of states ρ_N of the normal lead is constant in the energy window relevant for transport (wide-band approximation) and define the tunnel-coupling strength as $\Gamma_N = 2\pi \rho_N |V|^2$. The Hamiltonian of the resonator reads $H_{\text{osc}} = \hbar\omega_0 a^{\dagger} a$. The interaction Hamiltonian between the dot's degrees of freedom and the resonator is

$$H_{\text{int}} = \lambda (a^{\dagger} + a) \left(\sum_{\sigma} d_{\sigma}^{\dagger} d_{\sigma} - 1 \right), \quad (3)$$

where λ denotes the interaction strength. We have defined the equilibrium position of the oscillator when the dot is singly occupied. As shown in Appendix A, we decompose the charge-resonator interaction into a transverse part and a longitudinal part with respect to the Andreev states [36]. Then, using a polaronic transformation, the longitudinal interaction appears in the tunneling term [37]. The longitudinal part of the interaction on its own yields a nonequilibrium state of the resonator with an average energy larger than in the thermal state [38]. The inelastic tunneling processes associated with the longitudinal part scale as $\sim \lambda/(\hbar\omega_0)$ and can be safely neglected for $\lambda \ll \hbar\omega_0$. By contrast, the transversal coupling plays a crucial role even for $\lambda \ll \hbar\omega_0$. For small frequency detuning $|\hbar\omega_0 - 2\varepsilon_A| < \lambda$, the states of the system $|+, n\rangle$ and $|-, n+1\rangle$ are almost degenerate and get hybridized by the interaction even for $\lambda \ll \hbar\omega_0$. Hence, for the transverse interaction, we introduce the RWA, which is valid when $\hbar\omega_0 \approx (E_+ - E_-) = 2\varepsilon_A$. In the RWA the interaction Hamiltonian reads

$$H_{\text{int}}^{\text{RWA}} = \lambda \sin(2\theta) [a^{\dagger} |-\rangle \langle +| + a |+\rangle \langle -|]. \quad (4)$$

III. SEMICLASSICAL APPROXIMATION

We define the Hamiltonian of the system $H_s = H_{\text{dS}} + H_{\text{osc}} + H_{\text{int}}^{\text{RWA}}$. The reduced density matrix of the quantum dot coupled to the resonator ρ_s is obtained by tracing out the

normal lead, and it obeys the following Lindblad equation:

$$\hbar \frac{\partial \hat{\rho}_s}{\partial t} = -i[H_s, \rho_s] - \frac{\Gamma_N}{2} \sum_{\sigma} [\{d_{\sigma} d_{\sigma}^{\dagger}, \rho_s\} - 2d_{\sigma}^{\dagger} \rho_s d_{\sigma}] - \frac{\kappa}{2} [\{a^{\dagger} a, \rho_s\} - 2a \rho_s a^{\dagger}], \quad (5)$$

with $\{\cdot, \cdot\}$ being the anticommutator. The second term of the Lindblad equation (5) describes the single electron tunneling with the normal lead and is valid in the high-voltage regime with $eV > 0$, that is, when eV is much larger than all the other energy scales of the system (except the superconducting gap) [16]. The third term of Eq. (5) describes the relaxation of the resonator towards its ground state quantified by the rate κ/\hbar (namely, the intrinsic finite losses of the resonator).

Assuming that the resonator is in a lasing state, one can use the mean-field or semiclassical approximation in which we replace the bosonic operator a with its expectation value $a \approx \langle a \rangle = \alpha$. The quantity $|\alpha|^2$ represents, in the semiclassical language, the average number of bosons, i.e., $|\alpha|^2 \equiv A^2 \approx \langle a^{\dagger} a \rangle = \bar{n}$. In terms of the Fock states, the condition of validity for the semiclassical approximation reads $\bar{n} \gg \delta n$, with $\delta n = [(\langle a^{\dagger} a \rangle^2) - \bar{n}^2]^{1/2}$. Within the semiclassical approach, one can write a closed system of equations for the resonator amplitude α and the matrix elements of the reduced density matrix of the dot. More details are given in Appendix B. We focus on the resonant regime $\hbar\omega_0 = 2\epsilon_A$. The equation for the oscillator's energy dynamics is given by

$$\frac{\partial A^2}{\partial t} = \frac{1}{\hbar} [-\kappa - \gamma_{\text{eff}}(A^2)] A^2, \quad (6)$$

with

$$\gamma_{\text{eff}}(A^2) = -\frac{2\lambda^2 \sin^2(2\theta) \cos(2\theta)}{\Gamma_N} \frac{1}{1 + \frac{4\lambda^2 \sin^2(2\theta)}{\Gamma_N^2} A^2}. \quad (7)$$

Equations (6) and (7) are the mean-field semiclassical lasing equations [39]. They describe the laser as a classical oscillator with a simple linear friction (with damping coefficient κ) and a *nonlinear* gain which arises from the interaction with the two quantum levels. A nontrivial steady-state solution $\bar{A} \neq 0$ exists for coupling strength larger than the critical value $\lambda > \lambda_c$, which is known as the lasing threshold:

$$\lambda_c = \sqrt{\frac{\kappa \Gamma_N}{2}} \frac{[\delta^2 + \Gamma_S^2]^{3/4}}{\Gamma_S \sqrt{\delta}}, \quad \delta > 0. \quad (8)$$

Notice that lasing can be achieved only for $\delta > 0$ by choice of the applied voltage. If we invert the applied voltage, lasing occurs for $\delta < 0$. The solution for the amplitude in the semiclassical approach, which should be compared with \bar{n} , is

$$\bar{A}^2 = \left(\frac{\Gamma_N}{2\kappa} \right) \frac{\delta}{\sqrt{\delta^2 + \Gamma_S^2}} \left[1 - \left(\frac{\lambda_c}{\lambda} \right)^2 \right]. \quad (9)$$

IV. QUANTUM MASTER EQUATION IN RWA

In order to assess the relevance of quantum effects for single atom lasing in this system, we employ the quantum master-equation approach. We now use the basis $|s, n\rangle = |s\rangle \otimes |n\rangle$, where $s \in \{\uparrow, \downarrow, +, -\}$ labels the eigenstates of the

Hamiltonian in Eq. (1). Within the rotating-wave approximation the Hamiltonian H_s can be diagonalized. The states $|\sigma, n\rangle$ are eigenstates of H_s with eigenenergies $E_{\sigma, n} = \epsilon_0 + \hbar\omega_0 n$. In the presence of the interaction with the oscillator, the states $|\pm\rangle$ are hybridized with the Fock states, yielding the following eigenstates:

$$|rw+, n\rangle = \sin(\varphi_n)|+, n\rangle - \cos(\varphi_n)|-, n+1\rangle, \quad (10a)$$

$$|rw-, n\rangle = \cos(\varphi_n)|+, n\rangle + \sin(\varphi_n)|-, n+1\rangle, \quad (10b)$$

with $\sin(\varphi_n) = (1/\sqrt{2})[1 - \Delta/(2W_n)]^{1/2}$ and $\cos(\varphi_n) = (1/\sqrt{2})[1 + \Delta/(2W_n)]^{1/2}$, where $\Delta = \hbar\omega_0 - 2\epsilon_A$ is the detuning between states $|-, n+1\rangle$ and $|+, n\rangle$ and $W_n = [(\Delta/2)^2 + \lambda^2 \sin^2(2\theta)(n+1)]^{1/2}$. The eigenenergies corresponding to the eigenstates given in Eq. (10) are $E_{rw\pm, n} = E_{\pm} + \hbar\omega_0 n + \Delta/2 \pm W_n$.

Performing a perturbation expansion in H_{tun} , a master equation for the populations of the eigenstates of H_s can be obtained in the framework of a diagrammatic real-time technique [40,41]. Here we restrict ourselves to first order in Γ_N . We relabel the eigenstates of H_s as $|\alpha, n\rangle$, with $\alpha \in \{\uparrow, \downarrow, rw+, rw-\}$. The master equation for the occupation probabilities $P_{\alpha, n} = \text{Tr}_{\text{lead}}[\rho|\alpha, n\rangle\langle\alpha, n|]$ can be written as

$$\dot{P}_{\alpha, n} = \frac{1}{\hbar} \sum_{\alpha', n'} W_{(\alpha, n); (\alpha', n')} P_{\alpha', n'}, \quad (11)$$

where $W_{(\alpha, n); (\alpha', n')}/\hbar$ for $(\alpha', n') \neq (\alpha, n)$ is the transition rate from state $|\alpha', n'\rangle$ to $|\alpha, n\rangle$. The diagonal elements of the kernel $W_{(\alpha, n); (\alpha', n')}$ are defined by $W_{(\alpha, n); (\alpha, n)} = -\sum_{(\alpha', n') \neq (\alpha, n)} W_{(\alpha', n'); (\alpha, n)}$.

Using Fermi's golden rule, the transition rates associated with the tunneling events with the normal lead in the high-bias regime (unidirectional transport) are

$$W_{(\alpha, n); (\alpha', n')}^N(\chi) = \Gamma_N \sum_{\sigma} [e^{-i\chi} |\langle\alpha, n|d_{\sigma}^{\dagger}|\alpha', n'\rangle|^2], \quad (12)$$

where for ease of calculation we have introduced the counting field χ in the usual way [42]. The counting field allows us to express the current simply in terms of a derivative of a generalized transition rate. We introduce the damping of the resonator mode by coupling the oscillator to a zero-temperature bosonic bath. The corresponding rates are $W_{(\alpha, n); (\alpha', n')}^D = \kappa |\langle\alpha, n|a|\alpha', n'\rangle|^2$. The rates in the master equation (11) are given by $W_{(\alpha, n); (\alpha', n')} = W_{(\alpha, n); (\alpha', n')}^N(\chi) + W_{(\alpha, n); (\alpha', n')}^D$. The counting field χ needs to be removed from the diagonal elements of the kernel. The stationary probabilities $P_{\alpha, n}^{\text{stat}}$ are obtained solving Eq. (11) for $\dot{P}_{\alpha, n} = 0$ with the condition that $\sum_{\alpha, n} P_{\alpha, n} = 1$ and are the kernel of the matrix $W_{(\alpha, n); (\alpha', n')}$. The stationary current in the normal lead can be written in terms of the stationary probabilities as $I = -i \frac{e}{\hbar} \sum_{\alpha, \alpha', n, n'} \frac{\partial W_{(\alpha, n); (\alpha', n')}}{\partial \chi} \Big|_{\chi \rightarrow 0} P_{\alpha', n'}^{\text{stat}}$. To perform numerical computations, we introduce a maximum value n_{max} for the highest Fock state number with $n_{\text{max}} \gg \bar{n}$.

V. RESULTS AND DISCUSSION

In this section we present the results of the quantum master-equation approach in the RWA and compare them with

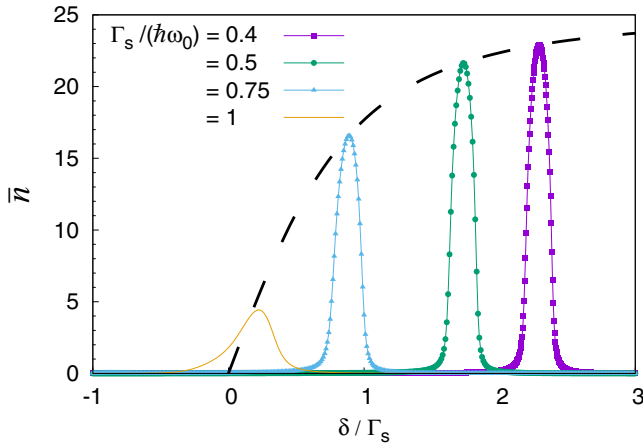


FIG. 2. Average occupation of the oscillator mode \bar{n} obtained by solution of the master equation as a function of the detuning $\delta = 2\varepsilon + U$ for different ratios of $\Gamma_S/(\hbar\omega_0)$. The dashed line corresponds to the semiclassical approximation, where the system is always on resonance. Parameters: $\lambda = 0.01 \hbar\omega_0$ and $\kappa/\Gamma_N = 0.02$.

the analytical results obtained by the semiclassical approximation.

A. Average occupation of the resonator

One of the telltales of lasing is a large average occupation of the resonator mode. The average occupation of the oscillator mode as a function of the detuning is shown in Fig. 2 together with the semiclassical result for small Γ_N , $\bar{n} = [\Gamma_N/(2\kappa)]\delta/[\delta^2 + \Gamma_S^2]^{1/2}$. As the semiclassical result corresponds to a situation where the parameters of the system are tuned to be always on resonance, it is an envelope to the curves corresponding to different values of Γ_S . Using the quantum master equation within the RWA, we find that \bar{n} shows a peak as a function of the detuning at $\delta^2 = (\hbar\omega_0)^2 - \Gamma_S^2$. The average occupation at the peak (on resonance) follows the semiclassical prediction, as can be seen in Fig 2.

We proceed by calculating the phase diagram of the system. In Fig. 3, we show a density plot of the average occupation of the resonator as a function of δ and of the coupling strength λ in Fig. 3(a) and of the tunneling strength Γ_S in Fig. 3(b). The occupation \bar{n} shows a peak located at $\delta^2 = (\hbar\omega_0)^2 - \Gamma_S^2$ with a width approximately given by $w = 4 \frac{\lambda\Gamma_S}{(\hbar\omega_0)} \sqrt{\bar{n}_{\text{res}} + 1}$, where $\bar{n}_{\text{res}} = [\Gamma_N/(2\kappa)]\sqrt{1 - \Gamma_S^2/(\hbar\omega_0)^2}$ is the occupation on resonance. The estimate of the width was obtained by looking at the range of values of δ for which $\sin(2\varphi_{\bar{n}_{\text{res}}})$ is different from zero. In Fig. 3(a), we notice that to this order in Γ_N there is no threshold when the system is perfectly on resonance, that is, $\Delta = \hbar\omega_0 - 2\varepsilon_A = 0$. However, this is true as long as $\Delta < \lambda$. Near the resonance, we see an increase of the occupation with increasing coupling strength λ . We do not show values of $\lambda > 0.1\hbar\omega$ as in this ultrastrong-coupling regime the RWA ceases to be valid.

B. Fano factor

In order to check whether the resonator is in a lasing state, we calculate the full Fock-state distribution p_n . The

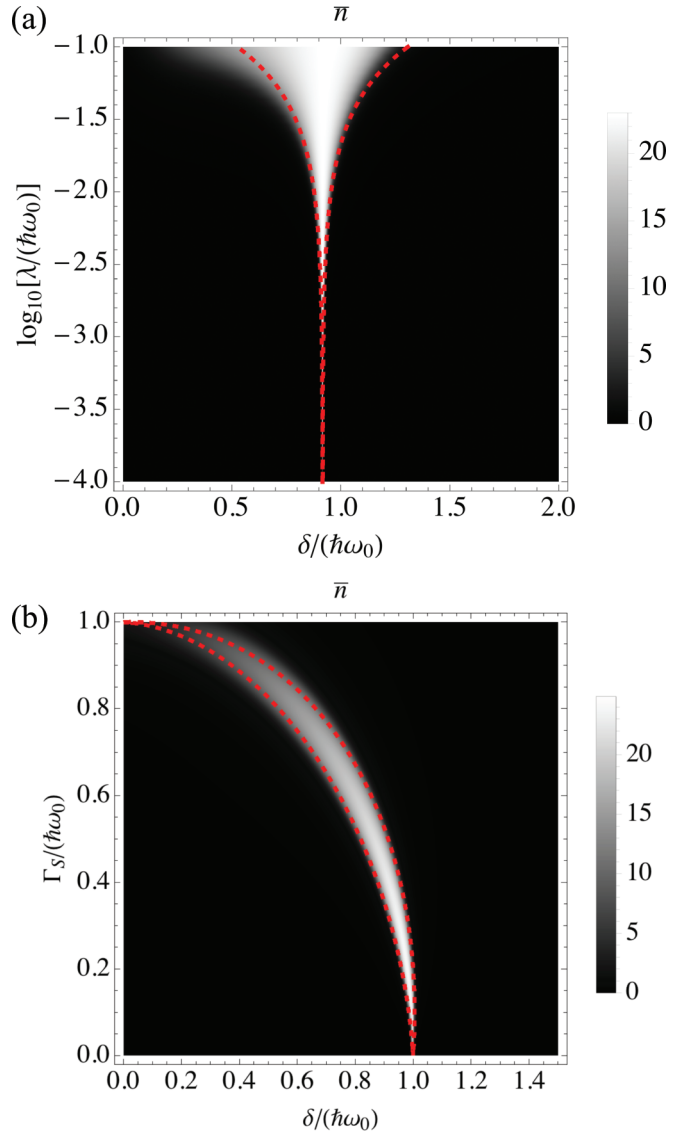


FIG. 3. (a) Density plot of the average bosonic occupation \bar{n} obtained by solution of the master equation as a function of $\delta/(\hbar\omega_0)$ and $\log_{10}[\lambda/(\hbar\omega_0)]$. Parameters: $\Gamma_S = 0.4 \hbar\omega_0$, $\kappa/\Gamma_N = 0.02$. (b) Density plot of the average bosonic occupation \bar{n} obtained by solution of the master equation as a function of $\delta/(\hbar\omega_0)$ and $\Gamma_S/(\hbar\omega_0)$. Parameters: $\lambda = 0.01 \hbar\omega_0$, $\kappa/\Gamma_N = 0.02$. The dashed lines in both panels correspond to the curves defined by $\delta - \sqrt{(\hbar\omega_0)^2 - \Gamma_S^2} \pm w/2 = 0$, with $w = 4 \frac{\lambda\Gamma_S}{(\hbar\omega_0)} \sqrt{\bar{n}_{\text{res}} + 1}$, and show the quality of the estimate for the width of the lasing region.

latter shows a peak centered at \bar{n} . To characterize the fluctuations around this peak, we introduce the Fano factor $F = [(\langle a^\dagger a \rangle^2) - \bar{n}^2]/\bar{n}$. The Fano factor as a function of detuning is shown in Fig. 4. Interestingly, F computed by the master-equation approach drops below 1 in the vicinity of the peak, clearly indicating sub-Poissonian lasing ($F < 1$). The semiclassical adiabatic approximation which is valid for ultralow damping, as discussed in Ref. [39], allows us to calculate the steady-state population of the Fock states and the Fano factor of the resonator F . For the present case, the adiabatic approximation, for coupling strengths larger than

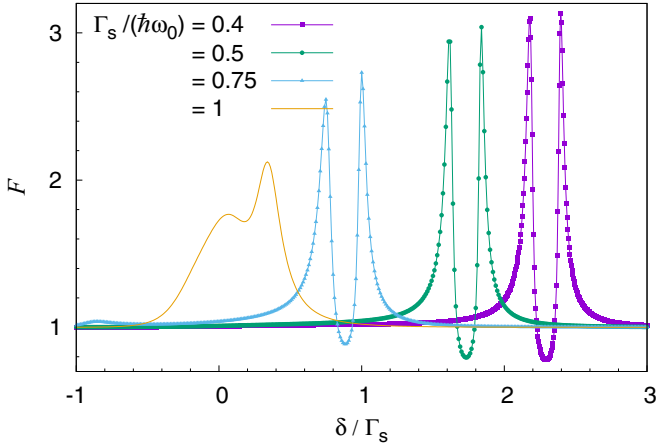


FIG. 4. Fano factor of the oscillator mode F obtained by solution of the master equation as a function of the detuning $\delta = 2\varepsilon + U$ for different ratios of $\Gamma_S/(\hbar\omega_0)$. Parameters: $\lambda = 0.01 \hbar\omega_0$ and $\kappa/\Gamma_N = 0.02$.

the threshold, yields $F \simeq 1$ on resonance. More details on the adiabatic approximation are given in Appendix B. We conclude that quantum fluctuations narrow the distribution p_n on resonance with respect to the Poissonian regime ($F = 1$), as was already found for different implementations of single atom lasers [43].

C. Transport current

In Fig. 5, we show the current as a function of the detuning. The current closely follows the result for zero coupling to the oscillator except on resonance, where it peaks at its maximum value achievable in the large-gap regime, i.e., $|e|\Gamma_N/\hbar$. The peak in the current indicates single atom lasing. The current behavior can be explained following the arguments of Ref. [42]. In the absence of coupling to the resonator, for

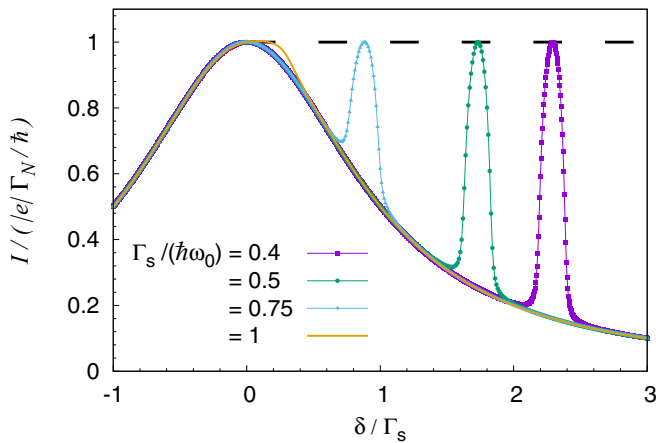


FIG. 5. Current flowing through the quantum dot obtained by the solution of the master equation. The current I is scaled with $|e|\Gamma_N/\hbar$ and is plotted as a function of the detuning $\delta = 2\varepsilon + U$ in units of Γ_S for different ratios of $\Gamma_S/(\hbar\omega_0)$. In the full lasing regime the current is pinned to the maximum value $|e|\Gamma_N/\hbar$ (dashed line). Parameters: $\lambda = 0.01 \hbar\omega_0$ and $\kappa/\Gamma_N = 0.02$.

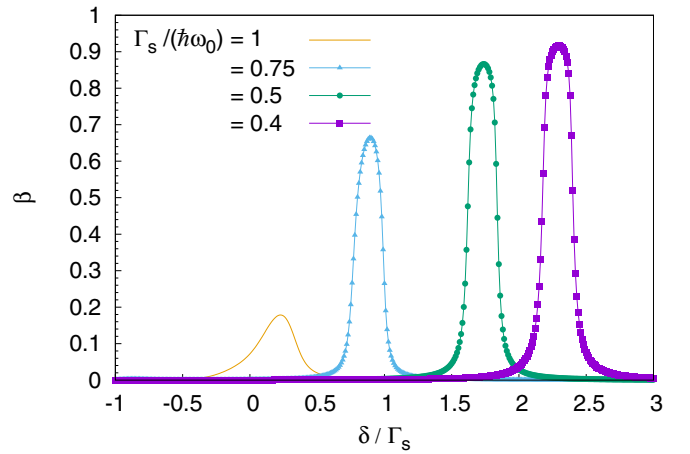


FIG. 6. Efficiency β as a function of δ/Γ_S for different ratios of $\Gamma_S/(\hbar\omega_0)$ obtained by the solution of the master equation. Parameters: $\lambda = 0.01 \hbar\omega_0$, $\kappa/\Gamma_N = 0.02$.

$\delta \gg \Gamma_S$ the dot will be mostly stuck in the state $|+\rangle \approx |D\rangle$, and the bottleneck for transport is the cotunneling of a Cooper pair to the superconductor with a rate $\propto \Gamma_S^2/\delta^2$ [refer also to Fig 1(d)]; this leads to a suppression of the current. The resonant coupling with the resonator removes this bottleneck by allowing the fast transition $|+, n\rangle \rightarrow |-, n+1\rangle \approx |0, n+1\rangle$. From state $|-, n+1\rangle$ a sequential tunneling event with the normal lead with rate $\propto \Gamma_N$ brings the dot in $|\sigma, n+1\rangle$ and a subsequent sequential tunneling event to $|+, n+1\rangle$ [see Fig. 1(e)]. In this case, the bottleneck for transport is the sequential tunneling with the normal lead, and the current reaches the same value as for $\delta = 0$ and no coupling to the oscillator. We wish to emphasize that the process which restores the maximum value of the current is the very same that leads to lasing.

D. Efficiency

We define the efficiency of the lasing mechanism as the number of quanta $\hbar\omega_0$ (photons) pumped into the resonator per transported Cooper pair. The efficiency is given by the ratio between the pumping photon flux and the Cooper-pair current flowing through the system $I/(2|e|)$. At steady state, the pumping photon flux into the cavity equals the output losses of the cavity, which read $\kappa\bar{n}/\hbar$. Hence, the efficiency is given by $\beta = \frac{\kappa\bar{n}/\hbar}{I/(2|e|)}$. In Fig. 6 we plot the efficiency β as obtained by means of the master equation in the RWA. On resonance, the efficiency is $\beta = \delta^2/\sqrt{\delta^2 + \Gamma_S^2} = \sqrt{1 - (\frac{\Gamma_S}{\hbar\omega_0})^2}$: the efficiency β reaches values in excess of 0.91 for $\Gamma_S/(\hbar\omega_0) < 0.4$.

E. Validity of the RWA and experimental feasibility

In order to validate the results obtained in the RWA we have employed the master-equation approach beyond the RWA approximation, that is, with the full interaction Hamiltonian of Eq. (3). In the parameter range explored in this paper, the results obtained with and without RWA agree extremely well, as shown in Appendix D.

Finally, an assessment of the experimental feasibility of the setup considered here is in order. Typical experimental

values are $\lambda/(2\pi\hbar) \sim 50\text{--}100$ MHz in single quantum dots [3] and $\omega_0/(2\pi) \sim 7$ GHz [3,5,31]. Large asymmetric tunnel coupling between the quantum dot and the superconductor has also been achieved [44], $\Gamma_N \ll \Gamma_S$. Γ_S can be tens of μeV , reaching the typical microwave cavity frequency [44] $\Gamma_S \lesssim \hbar\omega_0$. For computational reasons, we use a moderate damping coefficient for the intrinsic losses of the resonator. Experimental devices with a large quality factor can have better performance [31], viz., $Q = \hbar\omega_0/\kappa$, with $Q \sim 10^4$. For instance, at resonance $2\epsilon_A = \hbar\omega_0$, and assuming $\Gamma_S \sim \hbar\omega_0$, we have the scaling $\lambda_c/(\hbar\omega_0) \sim (1/\sqrt{Q})(\Gamma_N/\Gamma_S)^{1/2}$. In this case, one can estimate lasing even for smaller values of the coupling constant than the one used here ($\lambda = 0.01\hbar\omega_0$).

VI. CONCLUSIONS

In this paper we have shown that a quantum dot strongly coupled to a superconductor can implement a highly efficient single atom laser. Single atom lasing is achievable within the reach of the experimental state of the art for these hybrid nanodevices. Both a semiclassical treatment and a quantum master-equation approach have been employed to characterize the properties of this laser. We discuss the phase diagram and show that the Fock-state distribution on resonance is sub-Poissonian due to quantum effects. In the lasing state, the transport current through the quantum dot is pinned to the maximum value achievable in this hybrid nanostructure and hence can be used to identify the onset of lasing.

ACKNOWLEDGMENTS

G.R. is grateful for the warm hospitality at Victoria University of Wellington. G.R. thanks A. D. Armour for useful discussions and G. Burkard for relevant comments. G.R. and M.G. thank K. G. Steenbergen for suggested improvements to the manuscript. G.R. acknowledges partial support from the German Excellence Initiative through the Zukunftskolleg and from the Deutsche Forschungsgemeinschaft (DFG) through the collaborative research center SFB 767.

APPENDIX A: DERIVATION OF THE EFFECTIVE HAMILTONIAN IN THE ROTATING-WAVE APPROXIMATION

We consider the Hamiltonian

$$H = H_{\text{osc}} + H_{\text{int}} + H_{\text{dS}} + H_{\text{tun}} + H_N, \quad (\text{A1})$$

whose terms are described in the main text. The interaction Hamiltonian between the dot's degrees of freedom and the oscillator is

$$H_{\text{int}} = \lambda(a^\dagger + a) \left(\sum_{\sigma} d_{\sigma}^{\dagger} d_{\sigma} - 1 \right), \quad (\text{A2})$$

where λ denotes the interaction strength. The operator $\sum_{\sigma} d_{\sigma}^{\dagger} d_{\sigma} - 1$ can be expressed as

$$\sum_{\sigma} d_{\sigma}^{\dagger} d_{\sigma} - 1 = |D\rangle\langle D| - |0\rangle\langle 0| = \cos(2\theta)\tau_z + \sin(2\theta)\tau_x, \quad (\text{A3})$$

with $\tau_z = |+\rangle\langle +| - |-\rangle\langle -|$ and $\tau_x = |+\rangle\langle -| + |-\rangle\langle +|$. Hence, the interaction Hamiltonian reads

$$H_{\text{int}} = \lambda(a^\dagger + a)[\cos(2\theta)\tau_z + \sin(2\theta)\tau_x]. \quad (\text{A4})$$

We introduce the polaron transformation defined by the unitary operator $\hat{U}_z = e^{-iP\tau_z}$, with $P = -i[\lambda/(\hbar\omega_0)]\cos(2\theta)(a - a^\dagger)$. The transformed Hamiltonian reads

$$\begin{aligned} \hat{U}_z (H_{\text{osc}} + H_{\text{int}} + H_{\text{dS}}) \hat{U}_z^\dagger &= H_{\text{osc}} + H_{\text{dS}} - \frac{\lambda^2}{\hbar\omega_0} \cos^2(2\theta)[|+\rangle\langle +| + |-\rangle\langle -|] \\ &\quad + \lambda \sin(2\theta)[a + a^\dagger][e^{-2iP}|+\rangle\langle -| + e^{2iP}|-\rangle\langle +|] \\ &\quad - \frac{\lambda^2}{\hbar\omega_0} \sin(4\theta)\tau_z[e^{-2iP}|+\rangle\langle -| + e^{2iP}|-\rangle\langle +|]. \end{aligned} \quad (\text{A5})$$

The unitary transformation also changes the tunneling Hamiltonian, which contains the Fermionic operators of the dot. The latter operators can be written, for instance, as

$$\begin{aligned} d_{\uparrow} &= |0\rangle\langle \uparrow| + |\downarrow\rangle\langle D| = [-\sin(\theta)|+\rangle + \cos(\theta)|-\rangle]\langle \uparrow| \\ &\quad + |\downarrow\rangle[\cos(\theta)\langle +| + \sin(\theta)\langle -|], \end{aligned} \quad (\text{A6})$$

and we have

$$\begin{aligned} \hat{U}_z d_{\uparrow} \hat{U}_z^\dagger &= [-\sin(\theta)e^{-iP}|+\rangle + \cos(\theta)e^{iP}|-\rangle]\langle \uparrow| \\ &\quad + |\downarrow\rangle[\cos(\theta)e^{iP}\langle +| + \sin(\theta)e^{-iP}\langle -|]. \end{aligned} \quad (\text{A7})$$

A similar expression is valid for $\hat{U}_z d_{\downarrow} \hat{U}_z^\dagger$. Hereafter, we assume that we are working in the weak-coupling limit with $\lambda \ll \hbar\omega_0$, such that we can set the argument of the exponential function $P \simeq 0$ in Eqs. (A5) and (A7). Then the effective interaction reduces to

$$H_{\text{int}}^{(\text{eff})} = \lambda \sin(2\theta)[a + a^\dagger]\tau_x. \quad (\text{A8})$$

We define the Hamiltonian of the system as

$$H_s = H_{\text{osc}} + H_{\text{int}}^{(\text{eff})} + H_{\text{dS}}. \quad (\text{A9})$$

Finally, we introduce the rotating-wave approximation (RWA), which is valid when $\hbar\omega_0 \approx (E_+ - E_-) = 2\epsilon_A = \sqrt{\delta^2 + \Gamma_S^2}$, with the detuning $\Delta = \hbar\omega_0 - 2\epsilon_A$ satisfying the conditions $|\Delta| \ll \hbar\omega_0$, $|\Delta| \ll 2\epsilon_A$, and $|\Delta| \lesssim \lambda|\sin(2\theta)|$. In the RWA the interaction Hamiltonian reads

$$H_{\text{int}}^{\text{RWA}} = \lambda \sin(2\theta)[a^\dagger|-\rangle\langle +| + a|+\rangle\langle -|]. \quad (\text{A10})$$

In the presence of the interaction with the oscillator, the states $|\pm\rangle$ are hybridized with the Fock states. We now use the basis $|s, n\rangle = |s\rangle \otimes |n\rangle$, with $s \in \{\uparrow, \downarrow, +, -\}$ labeling the eigenstates of the effective Hamiltonian. In this basis, the interaction Hamiltonian reads

$$H_{\text{int}}^{\text{RWA}} = \lambda \sin(2\theta) \sum_{n=0}^{\infty} \sqrt{n+1}(|-, n+1\rangle\langle +, n| + \text{H.c.}). \quad (\text{A11})$$

APPENDIX B: ANALYTIC RESULTS FOR THE LASING IN RWA

From the Lindblad equation (5) of the main text, one can derive a hierarchy of coupled equations for the fermionic and bosonic operators which are generally not exactly solvable.

1. Semiclassical approximation

Assuming that the resonator is in a lasing state, one can use the mean-field or semiclassical approximation in which we replace the bosonic operator a with its expectation value $a \approx \langle a \rangle = \alpha$. Such an approximation is valid under the condition that the reduced density matrix of the resonator corresponds to a peaked distribution in phase-space representation, which is centered around the amplitude $|\alpha|$ with small quantum fluctuations. In other words we require the condition $|\alpha|^2 \gg \delta\alpha^2$, with $\delta\alpha^2 = \langle (a - \alpha)^2 \rangle$. For Poissonian fluctuations one has $\delta\alpha^2 \sim |\alpha|$, whereas $\delta\alpha^2 \sim |\alpha|^\nu$, with $\nu < 1$, for a sub-Poissonian distribution. Notice that in both cases the condition $|\alpha| \gg \delta\alpha$ is fulfilled. This condition defines the lasing state of the oscillator that we analyze here. The quantity $|\alpha|^2$ represents, in the semiclassical language, the average oscillator occupation $|\alpha|^2 = \alpha^* \alpha \approx \langle a^\dagger a \rangle = \bar{n}$.

Within the semiclassical approach, one can write a closed system of equations for the resonator amplitude α and the matrix elements of the reduced density matrix of the dot, namely, the populations p_+ , p_- , p_σ (diagonal elements) and the coherence factor ρ_{+-} for states $|\pm\rangle$ (off-diagonal element). The semiclassical equations read

$$\begin{aligned} \hbar \frac{\partial p_+}{\partial t} = & i\lambda \sin(2\theta)(\alpha + \alpha^*)(\rho_{+-} - \rho_{+-}^*) \\ & - \Gamma_N \left[2 \sin^2(\theta) p_+ - 2 \cos^2(\theta) p_\sigma \right. \\ & \left. + \frac{\sin(2\theta)}{2}(\rho_{+-} + \rho_{+-}^*) \right], \end{aligned} \quad (\text{B1})$$

$$\begin{aligned} \hbar \frac{\partial p_-}{\partial t} = & -i\lambda \sin(2\theta)(\alpha + \alpha^*)(\rho_{+-} - \rho_{+-}^*) \\ & - \Gamma_N \left[2 \cos^2(\theta) p_- - 2 \sin^2(\theta) p_\sigma \right. \\ & \left. + \frac{\sin(2\theta)}{2}(\rho_{+-} + \rho_{+-}^*) \right], \end{aligned} \quad (\text{B2})$$

$$\begin{aligned} \hbar \frac{\partial \rho_{+-}}{\partial t} = & -i(E_+ - E_-) - i\lambda \sin(2\theta)(\alpha + \alpha^*)(p_- - p_+) \\ & - \Gamma_N \left(\rho_{+-} + \frac{\sin(2\theta)}{2} \right), \end{aligned} \quad (\text{B3})$$

$$\begin{aligned} \hbar \frac{\partial p_\sigma}{\partial t} = & -\Gamma_N \left[p_\sigma - \sin^2(\theta) p_+ - \cos^2(\theta) p_- \right. \\ & \left. - \frac{\sin(2\theta)}{2}(\rho_{+-} + \rho_{+-}^*) \right]. \end{aligned} \quad (\text{B4})$$

Notice that the derivative of the sum $p_+ + p_- + 2p_\sigma$ vanishes; that is, the probability is conserved. The last equation in the semiclassical approach is for the oscillator's degree of freedom

$$\hbar \frac{\partial \alpha}{\partial t} = \left(-i\hbar\omega_0 - \frac{\kappa}{2} \right) \alpha - i\lambda \sin(2\theta)(\rho_{+-} + \rho_{+-}^*). \quad (\text{B5})$$

From the latter equation, we can obtain

$$\hbar \frac{\partial |\alpha|^2}{\partial t} = -\kappa |\alpha|^2 + i\lambda \sin(2\theta)(\rho_{+-} + \rho_{+-}^*)(\alpha - \alpha^*). \quad (\text{B6})$$

We now go into the rotating frame where the oscillator is at rest and set $\alpha(t) = \tilde{\alpha}(t)e^{-i\omega_0 t}$ and $\rho_{+-}(t) = \tilde{\rho}_{+-}(t)e^{-i\omega_0 t}$. Neglecting fast oscillating terms (RWA), at the resonance $\hbar\omega_0 = 2\epsilon_A$, we can write

$$\begin{aligned} \hbar \frac{\partial p_+}{\partial t} \simeq & i\lambda \sin(2\theta)(\tilde{\alpha}^* \rho_{+-} - \tilde{\alpha} \rho_{+-}^*) \\ & - \Gamma_N [2 \sin^2(\theta) p_+ - 2 \cos^2(\theta) p_\sigma], \end{aligned} \quad (\text{B7})$$

$$\begin{aligned} \hbar \frac{\partial p_-}{\partial t} \simeq & -i\lambda \sin(2\theta)(\tilde{\alpha}^* \rho_{+-} - \tilde{\alpha} \rho_{+-}^*) \\ & - \Gamma_N [2 \cos^2(\theta) p_- - 2 \sin^2(\theta) p_\sigma], \end{aligned} \quad (\text{B8})$$

$$\hbar \frac{\partial \tilde{\rho}_{+-}}{\partial t} \simeq -\Gamma_N \tilde{\rho}_{+-} - i\lambda \sin(2\theta) \tilde{\alpha} (p_- - p_+), \quad (\text{B9})$$

$$\hbar \frac{\partial p_\sigma}{\partial t} \simeq -\Gamma_N [p_\sigma - \sin^2(\theta) p_+ - \cos^2(\theta) p_-], \quad (\text{B10})$$

$$\hbar \frac{\partial |\alpha|^2}{\partial t} = -\kappa |\alpha|^2 + i\lambda \sin(2\theta)(\tilde{\alpha} \tilde{\rho}_{+-}^* - \tilde{\alpha}^* \tilde{\rho}_{+-}). \quad (\text{B11})$$

Using the normalization condition $p_+ + p_- + 2p_\sigma = 1$, the solutions for the populations read

$$p_+ = \frac{\cos^4(\theta) + \chi_{\tilde{\alpha}}}{1 + 4\chi_{\tilde{\alpha}}}, \quad (\text{B12})$$

$$p_- = \frac{\sin^4(\theta) + \chi_{\tilde{\alpha}}}{1 + 4\chi_{\tilde{\alpha}}}, \quad (\text{B13})$$

$$\tilde{\rho}_{+-} = \frac{i\lambda \sin(2\theta) \cos(2\theta)}{\Gamma_N} \left(\frac{\tilde{\alpha}}{1 + 4\chi_{\tilde{\alpha}}} \right), \quad (\text{B14})$$

with

$$\chi_{\tilde{\alpha}} = \frac{\lambda^2 \sin^2(2\theta)}{\Gamma_N^2} |\tilde{\alpha}|^2. \quad (\text{B15})$$

After setting $|\tilde{\alpha}|^2 = |\alpha|^2 = A^2$, the equation for the oscillator's energy dynamics is given by

$$\hbar \frac{\partial A^2}{\partial t} = [-\kappa - \gamma_{\text{eff}}(A^2)] A^2, \quad (\text{B16})$$

with

$$\gamma_{\text{eff}}(A^2) = -\frac{2\lambda^2}{\Gamma_N} \frac{\sin^2(2\theta) \cos(2\theta)}{1 + 4 \frac{\lambda^2 \sin^2(2\theta)}{\Gamma_N^2} A^2}. \quad (\text{B17})$$

Equations (B16) and (B17) are the mean-field semiclassical lasing equations. They describe the laser as a classical oscillator with simple linear friction (with damping coefficient κ) and a *negative, nonlinear* damping (gain) which arises from the interaction with the two quantum levels. A nontrivial solution $A \neq 0$ exists for coupling strengths larger than the critical value $\lambda > \lambda_c$, which is known as the lasing threshold:

$$\lambda_c = \sqrt{\frac{\kappa \Gamma_N}{2}} \frac{[\delta^2 + \Gamma_S^2]^{3/4}}{\Gamma_S \sqrt{\delta}}, \quad \delta > 0. \quad (\text{B18})$$

The solution for the amplitude A in the semiclassical approach, which should be compared with the average oscillator

occupation ($A^2 = |\alpha|^2 \approx \bar{n}$), is

$$\bar{A}^2 = \left(\frac{\Gamma_N}{2\kappa} \right) \frac{\delta}{\sqrt{\delta^2 + \Gamma_S^2}} \left[1 - \left(\frac{\lambda_c}{\lambda} \right)^2 \right]. \quad (\text{B19})$$

2. Adiabatic approximation on resonance: Effective equation for p_n

Starting from the Lindblad equation (5) of the main text, we perform the so-called adiabatic approximation, which is valid for ultralow damping [39] defined by the conditions $\kappa \ll \Gamma_N$ and $\kappa \ll \lambda \sin(2\theta)$. In other words, the intrinsic relaxation of the resonator (e.g., due to the coupling to a thermal bath) is assumed to be very slow compared to the

internal dynamics of the systems and the timescale associated with tunneling with the normal lead.

Along the lines of Ref. [39], one can find the steady-state population p_n of the Fock states of the resonator in the ultraunderdamped regime of the resonator.

We use the interaction representation for the density matrix of the system formed by the oscillator and the proximized dot. We set $\rho(t) = e^{-\frac{i}{\hbar}H_0 t} \rho_I(t) e^{\frac{i}{\hbar}H_0 t}$, with $H_0 = H_{\text{osc}} + H_{\text{ds}}$ and $\rho_I(t)$ being the density matrix in interaction picture. For the sake of conciseness, we adopt the notation

$$\lambda_T = \lambda \sin(2\theta). \quad (\text{B20})$$

Using the RWA, the matrix elements of ρ_I satisfy the following (exact) equations:

$$\begin{aligned} \hbar \dot{\rho}_{nm}^{++} = & -i\lambda_T(\sqrt{n+1}\rho_{n+1m}^{+-} - \sqrt{m+1}\rho_{nm+1}^{+-}) - 2\Gamma_N[\sin^2(\theta)\rho_{nm}^{++} - \cos^2(\theta)\rho_{nm}^{\sigma\sigma}] \\ & - \frac{\kappa}{2}[(n+m)\rho_{nm}^{++} - 2\sqrt{(n+1)(m+1)}\rho_{n+1m+1}^{++}], \end{aligned} \quad (\text{B21})$$

$$\hbar \dot{\rho}_{nm}^{--} = i\lambda_T(\sqrt{m}\rho_{nm-1}^{+-} - \sqrt{n}\rho_{n-1m}^{+-}) - 2\Gamma_N[\cos^2(\theta)\rho_{nm}^{--} - \sin^2(\theta)\rho_{nm}^{\sigma\sigma}] - \frac{\kappa}{2}[(n+m)\rho_{nm}^{--} - 2\sqrt{(n+1)(m+1)}\rho_{n+1m+1}^{--}], \quad (\text{B22})$$

$$\hbar \dot{\rho}_{nm}^{-+} = -i\lambda_T(\sqrt{n}\rho_{n-1m}^{+-} - \sqrt{m+1}\rho_{nm+1}^{+-}) - \Gamma_N\rho_{nm}^{-+} - \frac{\kappa}{2}[(n+m)\rho_{nm}^{-+} - 2\sqrt{(n+1)(m+1)}\rho_{n+1m+1}^{-+}], \quad (\text{B23})$$

$$\hbar \dot{\rho}_{nm}^{+-} = i\lambda_T(\sqrt{m}\rho_{nm-1}^{+-} - \sqrt{n+1}\rho_{n+1m}^{+-}) - \Gamma_N\rho_{nm}^{+-} - \frac{\kappa}{2}[(n+m)\rho_{nm}^{+-} - 2\sqrt{(n+1)(m+1)}\rho_{n+1m+1}^{+-}], \quad (\text{B24})$$

$$\hbar \dot{\rho}_{nm}^{\sigma\sigma} = -\Gamma_N[\rho_{nm}^{\sigma\sigma} - \sin^2(\theta)\rho_{nm}^{++} - \cos^2(\theta)\rho_{nm}^{--}] - \frac{\kappa}{2}[(n+m)\rho_{nm}^{\sigma\sigma} - 2\sqrt{(n+1)(m+1)}\rho_{n+1m+1}^{\sigma\sigma}]. \quad (\text{B25})$$

The above set of equations is not in a closed form. In the limit of the ultraunderdamping regime of the resonator, one can neglect the relaxation dynamics due to the interaction with the thermal bath since this occurs on a longer timescale than the dynamics associated with the single electron tunneling and the coherent coupling between the resonator and the two levels $|+\rangle$ and $|-\rangle$. This is the so-called adiabatic approximation [39], where the terms proportional to κ can be neglected. Using this approximation and relabeling the diagonal elements as populations $\rho_{nm}^{++} = p_n^+$, $\rho_{n+1,n+1}^{--} = p_{n+1}^-$, and $\rho_{mm}^{\sigma\sigma} = p_m^\sigma$, we can write the following closed system of equations for the steady state:

$$\begin{aligned} 0 = & -i\lambda_T\sqrt{n+1}(\rho_{n+1,n}^{+-} - \rho_{n,n+1}^{+-}) \\ & - 2\Gamma_N[\sin^2(\theta)p_n^+ - \cos^2(\theta)p_n^\sigma], \end{aligned} \quad (\text{B26})$$

$$\begin{aligned} 0 = & i\lambda_T\sqrt{n+1}(\rho_{n+1,n}^{+-} - \rho_{n,n+1}^{+-}) \\ & - 2\Gamma_N[\cos^2(\theta)p_{n+1}^- \sin^2(\theta)p_{n+1}^\sigma], \end{aligned} \quad (\text{B27})$$

$$0 = -i\lambda_T\sqrt{n+1}(p_n^+ - p_{n+1}^-) - \Gamma_N\rho_{n+1,n}^{+-}, \quad (\text{B28})$$

$$0 = i\lambda_T\sqrt{n+1}(p_n^+ - p_{n+1}^-) - \Gamma_N\rho_{n,n+1}^{+-}. \quad (\text{B29})$$

The equations for the populations with the dot being singly occupied read

$$p_n^\sigma = \sin^2(\theta)p_n^+ + \cos^2(\theta)p_n^-, \quad (\text{B30})$$

$$p_{n+1}^\sigma = \sin^2(\theta)p_{n+1}^+ + \cos^2(\theta)p_{n+1}^-. \quad (\text{B31})$$

Now, we introduce the reduced density matrix of the resonator defined by summing over the dot's states. In particular, the distribution for the populations of the Fock states p_n is given by

$$p_n = p_n^+ + p_n^- + 2p_n^\sigma, \quad (\text{B32})$$

$$p_{n+1} = p_{n+1}^+ + p_{n+1}^- + 2p_{n+1}^\sigma. \quad (\text{B33})$$

From Eqs. (B30), (B31), (B32), and (B33) one obtains

$$p_n^\sigma = \frac{[\sin^2(\theta) - \cos^2(\theta)]p_n^+ + \cos^2(\theta)p_n^-}{1 + 2\cos^2(\theta)}, \quad (\text{B34})$$

$$p_{n+1}^\sigma = \frac{[\cos^2(\theta) - \sin^2(\theta)]p_{n+1}^- + \sin^2(\theta)p_{n+1}^+}{1 + 2\sin^2(\theta)}. \quad (\text{B35})$$

Inserting Eqs. (B34) and (B35) into (B26) and (B27), we solve the full set of Eqs. (B26), (B27), (B28), and (B29) and find the steady-state solutions for p_n^+ , p_{n+1}^- , $\rho_{n+1,n}^{+-}$, and $\rho_{n,n+1}^{+-}$. In particular one obtains the following result:

$$\begin{aligned} \mathcal{A}_{n+1} = & -i\lambda_T\sqrt{n+1}(\rho_{n+1,n}^{+-} - \rho_{n,n+1}^{+-}) \\ = & \frac{2\Gamma_N\lambda_T^2(n+1)}{\Gamma_N^2 + 4\lambda_T^2(n+1)}[\cos^4(\theta)p_n - \sin^4(\theta)p_{n+1}]. \end{aligned} \quad (\text{B36})$$

Equation (B36) represents the gain rate of the laser, and it is the crucial result to derive the effective equation for p_n . The equation for the reduced density matrix of the resonator with matrix element $\rho_{n,m}$, in the interaction picture, is obtained by

tracing over the dot's states,

$$\begin{aligned} \hbar \dot{\rho}_{nm} = & -i\lambda_T(\sqrt{n+1}\rho_{n+1m}^- - \sqrt{m+1}\rho_{nm+1}^+) \\ & + i\lambda_T(\sqrt{m}\rho_{nm-1}^- - \sqrt{n}\rho_{n-1m}^+) \\ & - \frac{\kappa}{2}[(n+m)\rho_{nm} - 2\sqrt{(n+1)(m+1)}\rho_{n+1m+1}]. \end{aligned} \quad (\text{B37})$$

For the population $p_n = \rho_{nn}$ we have

$$\hbar \dot{p}_n = \mathcal{A}_{n+1} - \mathcal{A}_n - \kappa[np_n - (n+1)p_{n+1}]. \quad (\text{B38})$$

Inserting Eq. (B36) into Eq. (B38), one obtains the steady-state solution under the condition of detailed balance,

$$0 = \left(\kappa n + \frac{2\Gamma_N \lambda_T^2 \sin^4(\theta)}{\Gamma_N^2 + 4\lambda_T^2 n} n \right) p_n - \frac{2\Gamma_N \lambda_T^2 \cos^4(\theta)}{\Gamma_N^2 + 4\lambda_T^2 n} n p_{n-1}. \quad (\text{B39})$$

The iterative solution reads

$$p_n = \frac{a_c}{b_c + n} p_{n-1}, \quad (\text{B40})$$

with

$$a_c = \frac{\Gamma_N}{2\kappa} \cos^4(\theta), \quad b_c = \frac{\Gamma_N}{2\kappa} \sin^4(\theta) + \frac{\Gamma_N^2}{4\lambda \sin^2(2\theta)}. \quad (\text{B41})$$

The normalized solution of Eq. (B40) reads

$$p_n = b_c \frac{a_c^n}{(b_c)_{(n+1)}} p_0, \quad p_0 = \frac{1}{{}_1F_1(1, 1 + b_c, a_c)}, \quad (\text{B42})$$

with the generalized hypergeometric function ${}_1F_1$ defined as

$${}_1F_1(x, y; z) = \sum_{n=0}^{\infty} \frac{z^n}{n!} \frac{(x)_n}{(y)_n} \quad (\text{B43})$$

and where $(\dots)_n$ is the Pochhammer symbol, defined by

$$(x)_n = x(x+1)\cdots(x+n-2)(x+n-1) = \frac{\Gamma(x+n)}{\Gamma(x)}. \quad (\text{B44})$$

By calculating the average number $\langle n \rangle$, we obtain

$$\langle n \rangle = \bar{n} = \sum_{n=1}^{\infty} n p_n = a_c - b_c(1 - p_0). \quad (\text{B45})$$

In the limit of $\lambda \rightarrow \infty$, one recovers the result $\bar{n} \approx \Gamma_N/(2\kappa)$ (in this limit $p_0 \approx 0$). For the average of n^2 we find

$$\langle n^2 \rangle = \sum_{n=1}^{\infty} n^2 p_n = \bar{n}(a_c - b_c) + a_c, \quad (\text{B46})$$

and the Fano factor is given by

$$F = \frac{\langle n^2 \rangle - \bar{n}^2}{\bar{n}} = \frac{a_c}{a_c - b_c(1 - p_0)} - b p_0. \quad (\text{B47})$$

Inserting Eq. (B41) into Eq. (B47), one obtains $F \approx 1$ above the lasing threshold $\lambda \gg \lambda_c$.

APPENDIX C: MASTER EQUATION IN RWA

Within the rotating-wave approximation the Hamiltonian $H_{\text{dS}} + H_{\text{osc}} + H_{\text{int}}^{\text{RWA}}$ can be diagonalized. The eigenstates read

$$|\sigma, n\rangle, \quad (\text{C1a})$$

$$|rw+, n\rangle = \sin(\varphi_n)|+, n\rangle - \cos(\varphi_n)|-, n+1\rangle, \quad (\text{C1b})$$

$$|rw-, n\rangle = \cos(\varphi_n)|+, n\rangle + \sin(\varphi_n)|-, n+1\rangle, \quad (\text{C1c})$$

with

$$\sin(\varphi_n) = \frac{1}{\sqrt{2}} \sqrt{1 - \frac{\Delta/2}{W_n}}, \quad (\text{C2a})$$

$$\cos(\varphi_n) = \frac{1}{\sqrt{2}} \sqrt{1 + \frac{\Delta/2}{W_n}}, \quad (\text{C2b})$$

where $\Delta = \hbar\omega_0 - 2\epsilon_A$ is the detuning between states $|-, n+1\rangle$ and $|+, n\rangle$ and $W_n = \sqrt{(\frac{\Delta}{2})^2 + \lambda^2 \sin^2(2\theta)(n+1)}$. The eigenenergies corresponding to the eigenstates (C1) are

$$E_{\sigma, n} = \epsilon_0 + \hbar\omega_0 n, \quad (\text{C3a})$$

$$E_{rw\pm, n} = E_+ + \hbar\omega_0 n + \frac{\Delta}{2} \pm W_n. \quad (\text{C3b})$$

We now wish to obtain the occupation probabilities for the eigenstates (C1) of the RWA Hamiltonian, $P_{\alpha, n} = \text{Tr}_{\text{lead}}[\rho|\alpha, n\rangle\langle\alpha, n|]$, with ρ being the density matrix of the system and $\alpha \in \{\uparrow, \downarrow, rw+, rw-\}$. Performing a perturbation expansion in H_{tunn} , either in the Lindblad-equation formalism or in the framework of a diagrammatic real-time technique [40,41], yields the master equation

$$\dot{P}_{\alpha, n} = \frac{1}{\hbar} \sum_{\alpha', n'} W_{(\alpha, n); (\alpha', n')} P_{\alpha', n'}. \quad (\text{C4})$$

Since we restrict our calculation to first order in the tunnel coupling with the normal lead Γ_N , the rates can be calculated by means of Fermi's golden rule:

$$\begin{aligned} W_{(\alpha, n); (\alpha', n')}^N(\chi) &= \Gamma_N \sum_{\sigma} \{ e^{-i\chi} f(E_{\alpha, n} - E_{\alpha', n'}) |\langle\alpha, n|d_{\sigma}^{\dagger}|\alpha', n'\rangle|^2 \\ &+ e^{i\chi} [1 - f(E_{\alpha', n'} - E_{\alpha, n})] |\langle\alpha, n|d_{\sigma}|\alpha', n'\rangle|^2 \}, \end{aligned} \quad (\text{C5})$$

where χ is the counting field for electrons entering the normal lead [42] and $f(\epsilon) = \{1 + \exp[(\epsilon - \mu_N)/k_B T]\}^{-1}$ denotes the Fermi function of the normal lead, with $\mu_N = eV$ being the chemical potential and T being the temperature. In the high-bias regime, the electron transport is unidirectional, and the golden-rule rates simplify to

$$W_{(\alpha, n); (\alpha', n')}^N(\chi) = \Gamma_N \sum_{\sigma} [e^{-i\chi} |\langle\alpha, n|d_{\sigma}^{\dagger}|\alpha', n'\rangle|^2]. \quad (\text{C6})$$

The matrix elements in the rates are easy to evaluate. The nonvanishing matrix elements read

$$\begin{aligned} \langle\sigma, n|d_{\sigma}^{\dagger}|rw+, n'\rangle &= \delta_{n', n} \sin(\theta) \sin(\varphi_n) \\ &- \delta_{n', n-1} \cos(\theta) \cos(\varphi_{n-1}), \end{aligned} \quad (\text{C7a})$$

$$\langle \sigma, n | d_\sigma^\dagger | r w -, n' \rangle = \delta_{n',n} \sin(\theta) \cos(\varphi_{n-1}) + \delta_{n',n-1} \cos(\theta) \sin(\varphi_{n-1}). \quad (\text{C7b})$$

We now introduce some damping of the oscillator's mode. This is done by coupling the oscillator to a bosonic bath. We will consider an interaction Hamiltonian of the form

$$H_{\text{damp}} = -k_d \sum_i (b_i^\dagger a + a^\dagger b_i). \quad (\text{C8})$$

Furthermore, we will assume that the bosonic bath is at zero temperature (namely, $k_B T \ll \hbar \omega_0$). Therefore, only the terms $b_i^\dagger a$ will cause transitions. The transition rates due to the dissipative bath are

$$W_{(\alpha,n);(\alpha',n')}^D = \kappa |\langle \alpha, n | a | \alpha', n' \rangle|^2, \quad (\text{C9})$$

where we have introduced the coupling strength $\kappa \propto |k_d|^2$.

The off-diagonal rates $[(\alpha, n) \neq (\alpha', n')]$ in the master equation (C4) are given by

$$W_{(\alpha,n);(\alpha',n')}^N = W_{(\alpha,n);(\alpha',n')}^N(\chi) + W_{(\alpha,n);(\alpha',n')}^D, \quad (\text{C10})$$

and the diagonal elements are given by

$$W_{(\alpha,n);(\alpha,n)} = - \sum_{(\alpha',n') \neq (\alpha,n)} [W_{(\alpha',n');(\alpha,n)}^N(\chi = 0) + W_{(\alpha',n');(\alpha,n)}^D]. \quad (\text{C11})$$

In order to perform numerical calculations we truncate the Hilbert space by introducing a maximum value n_{max} for the quantum number of the oscillator. The dimension of the truncated Hilbert space is $4(n_{\text{max}} + 1)$. The master equation (C4) can therefore be written in matrix form as

$$\dot{\mathbf{P}} = \mathbf{W} \mathbf{P}, \quad (\text{C12})$$

where \mathbf{W} is a $4(n_{\text{max}} + 1) \times 4(n_{\text{max}} + 1)$ matrix. We define a vector containing all probabilities as

$$\mathbf{P} = (P_{-,0}, \mathbf{p}_0, \mathbf{p}_1, \dots, \mathbf{p}_n, \dots, \mathbf{p}_{n_{\text{max}}-1}, P_{\uparrow, n_{\text{max}}}, P_{\downarrow, n_{\text{max}}}, P_{+, n_{\text{max}}})^T, \quad (\text{C13})$$

with

$$\mathbf{p}_n = (P_{\uparrow, n}, P_{\downarrow, n}, P_{rw+, n}, P_{rw-, n})^T. \quad (\text{C14})$$

Notice that the state $|-, 0\rangle$, which is not coupled to other states by $H_{\text{int}}^{\text{RWA}}$, also needs to be included. Similarly, in the sector with $n = n_{\text{max}}$, the state $|+, n_{\text{max}}\rangle$ is not coupled to any other state due to the truncation of the Hilbert space of the oscillator. The vector of the stationary probabilities \mathbf{P}^{stat} is the null space of the matrix \mathbf{W} . Once we have obtained the probabilities, we can easily calculate other stationary properties, such as the current flowing in the normal lead and the Fock distribution of the oscillator. The full Fock-state distribution for the on-resonance case is shown in Fig. 7(a), and it is compared with the result of the adiabatic expansion, Eq. (B42)

APPENDIX D: MASTER EQUATION BEYOND RWA

We now wish to go beyond the RWA and consider the full Hamiltonian H_{int} of Eq. (A2). To this purpose we diagonalize $H_{\text{dS}} + H_{\text{osc}} + H_{\text{int}}$ numerically in the truncated $4(n_{\text{max}} + 1)$ -dimensional Hilbert space. We use as a basis $|s, n\rangle = |s\rangle \otimes$

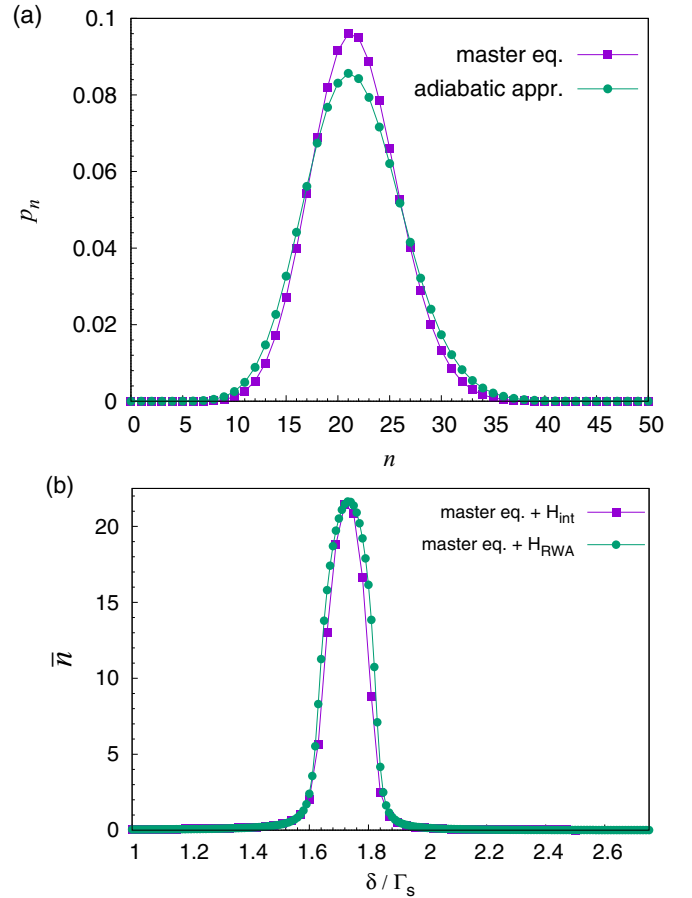


FIG. 7. (a) The probabilities p_n , namely, the distribution of the Fock states of the resonator, in the high-voltage regime obtained numerically by means of the quantum master equation within the RWA (squares) and the analytic results, Eq. (B42), within the adiabatic approximation (dots). The detuning corresponds to the on-resonance condition. (b) Comparison between the results obtained by the master equation with and without the RWA for the average occupation of the oscillator mode \bar{n} as a function of the detuning $\delta = 2\varepsilon_0 + U$ in units of Γ_S . Parameters for (a) and (b): $\Gamma_S = 0.5\hbar\omega_0$, $\lambda = 0.01\hbar\omega_0$, $\kappa/\Gamma_N = 0.02$, and the numerical cutoff $n_{\text{max}} = 100$.

$|n\rangle$, with $s \in \{\uparrow, \downarrow, +, -\}$. The eigenenergies are denoted by E_l , and the corresponding eigenstates are written as

$$|E_l\rangle = \sum_{s,n} a_{l;s,n} |s, n\rangle. \quad (\text{D1})$$

Notice that the eigenstates with the dot singly occupied are simply $|\sigma, n\rangle$. Using the states in Eq. (D1) as a basis, the rates can be written, in the high-bias voltage limit, as

$$W_{l;m}^N(\chi) = \Gamma \sum_{\sigma} [e^{-i\chi} \langle E_l | d_{\sigma}^{\dagger} | E_m \rangle]^2, \quad (\text{D2})$$

$$W_{l;m}^D = \kappa \sum_{\sigma} [|\langle E_l | a | E_m \rangle|^2]. \quad (\text{D3})$$

The results obtained without the RWA agree extremely well with those obtained within the RWA, as shown in Fig. 7(b). The average occupation of the resonator as a function of the detuning computed both with and without RWA are in almost

perfect agreement. The Fock distributions p_n on resonance, computed with both methods (not shown), are practically

indistinguishable. This establishes the validity of the results of the RWA.

-
- [1] J. J. Viennot, M. C. Dartiailh, A. Cottet, and T. Kontos, Coherent coupling of a single spin to microwave cavity photons, *Science* **349**, 408 (2015).
- [2] A. Stockklauser, V. F. Maisi, J. Basset, K. Cujia, C. Reichl, W. Wegscheider, T. Ihn, A. Wallraff, and K. Ensslin, Microwave Emission from Hybridized States in a Semiconductor Charge Qubit, *Phys. Rev. Lett.* **115**, 046802 (2015).
- [3] L. E. Bruhat, J. J. Viennot, M. C. Dartiailh, M. M. Desjardins, T. Kontos, and A. Cottet, Cavity Photons as a Probe for Charge Relaxation Resistance and Photon Emission in a Quantum Dot Coupled to Normal and Superconducting Continua, *Phys. Rev. X* **6**, 021014 (2016).
- [4] X. Mi, J. V. Cady, D. M. Zajac, P. W. Deelman, and J. R. Petta, Strong coupling of a single electron in silicon to a microwave photon, *Science* **355**, 156 (2016).
- [5] A. Stockklauser, P. Scarlino, J. V. Koski, S. Gasparinetti, C. K. Andersen, C. Reichl, W. Wegscheider, T. Ihn, K. Ensslin, and A. Wallraff, Strong Coupling Cavity QED with Gate-Defined Double Quantum Dots Enabled by a High Impedance Resonator, *Phys. Rev. X* **7**, 011030 (2017).
- [6] Y. Li, S.-X. Li, F. Gao, H.-O. Li, G. Xu, K. Wang, D. Liu, G. Cao, M. Xiao, T. Wang, J.-J. Zhang, G.-C. Guo, and G.-P. Guo, Coupling a germanium hut wire hole quantum dot to a superconducting microwave resonator, *Nano Lett.* **18**, 2091 (2018).
- [7] A. Benyamini, A. Hamo, S. V. Kusminskiy, F. von Oppen, and S. Ilani, Real-space tailoring of the electron-phonon coupling in ultraclean nanotube mechanical resonators, *Nat. Phys.* **10**, 151 (2014).
- [8] Y. Okazaki, I. Mahboob, K. Onomitsu, S. Sasaki, and H. Yamaguchi, Gate-controlled electromechanical backaction induced by a quantum dot, *Nat. Commun.* **7**, 11132 (2016).
- [9] G.-W. Deng, D. Zhu, X.-H. Wang, C.-L. Zou, J.-T. Wang, H.-O. Li, G. Cao, D. Liu, Y. Li, M. Xiao, G.-C. Guo, K.-L. Jiang, X.-C. Dai, and G.-P. Guo, Strongly coupled nanotube electromechanical resonators, *Nano Letters* **16**, 5456 (2016).
- [10] C. Urgell, W. Yang, S. L. de Bonis, C. Samanta, M. J. Esplandiu, Q. Dong, Y. Jin, and A. Bachtold, Cooling and self-oscillation in a nanotube electro-mechanical resonator, [arXiv:1903.04892](https://arxiv.org/abs/1903.04892).
- [11] Y. Wen, N. Ares, F. J. Schupp, T. Pei, G. A. D. Briggs, and E. A. Laird, A coherent nanomechanical oscillator driven by single-electron tunnelling, [arXiv:1903.04474](https://arxiv.org/abs/1903.04474).
- [12] H. Walther, B. T. H. Varcoe, B.-G. Englert, and T. Becker, Cavity quantum electrodynamics, *Rep. Prog. Phys.* **69**, 1325 (2006).
- [13] O. Astafiev, K. Inomata, A. O. Niskanen, T. Yamamoto, Y. A. Pashkin, Y. Nakamura, and J. S. Tsai, Single artificial-atom lasing, *Nature (London)* **449**, 588 (2007).
- [14] D. A. Rodrigues, J. Imbers, and A. D. Armour, Quantum Dynamics of a Resonator Driven by a Superconducting Single-Electron Transistor: A Solid-State Analogue of the Micromaser, *Phys. Rev. Lett.* **98**, 067204 (2007).
- [15] D. A. Rodrigues, J. Imbers, T. J. Harvey, and A. D. Armour, Dynamical instabilities of a resonator driven by a superconducting single-electron transistor, *New J. Phys.* **9**, 84 (2007).
- [16] M. Mantovani, A. D. Armour, W. Belzig, and G. Rastelli, Dynamical multistability in a quantum-dot laser, *Phys. Rev. B* **99**, 045442 (2019).
- [17] P. D. Nation, Nonclassical mechanical states in an optomechanical micromaser analog, *Phys. Rev. A* **88**, 053828 (2013).
- [18] N. Lambert, F. Nori, and C. Flindt, Bistable Photon Emission from a Solid-State Single-Atom Laser, *Phys. Rev. Lett.* **115**, 216803 (2015).
- [19] S.-N. Zhang, W. Pei, T.-F. Fang, and Q.-f. Sun, Phonon-assisted transport through quantum dots with normal and superconducting leads, *Phys. Rev. B* **86**, 104513 (2012).
- [20] A. Cottet, T. Kontos, and A. L. Yeyati, Subradiant Split Cooper Pairs, *Phys. Rev. Lett.* **108**, 166803 (2012).
- [21] J. R. Souquet, M. J. Woolley, J. Gabelli, P. Simon, and A. A. Clerk, Photon-assisted tunneling with nonclassical light, *Nat. Commun.* **5**, 5562 (2014).
- [22] P. Stadler, W. Belzig, and G. Rastelli, Ground-State Cooling of a Mechanical Oscillator by Interference in Andreev Reflection, *Phys. Rev. Lett.* **117**, 197202 (2016).
- [23] P. Stadler, W. Belzig, and G. Rastelli, Charge-vibration interaction effects in normal-superconductor quantum dots, *Phys. Rev. B* **96**, 045429 (2017).
- [24] L. Arrachea, N. Bode, and F. von Oppen, Vibrational cooling and thermoelectric response of nanoelectromechanical systems, *Phys. Rev. B* **90**, 125450 (2014).
- [25] M. Mantovani, W. Belzig, G. Rastelli, and R. Hussein, Single-photon pump by Cooper-pair splitting, [arXiv:1907.04308](https://arxiv.org/abs/1907.04308).
- [26] W. T. Morley, A. Di Marco, M. Mantovani, P. Stadler, W. Belzig, G. Rastelli, and A. D. Armour, Theory of double Cooper-pair tunneling and light emission mediated by a resonator, *Phys. Rev. B.* (to be published).
- [27] L. Childress, A. S. Sørensen, and M. D. Lukin, Mesoscopic cavity quantum electrodynamics with quantum dots, *Phys. Rev. A* **69**, 042302 (2004).
- [28] P.-Q. Jin, M. Marthaler, J. H. Cole, A. Shnirman, and G. Schön, Lasing and transport in a quantum-dot resonator circuit, *Phys. Rev. B* **84**, 035322 (2011).
- [29] M. Kulkarni, O. Cotlet, and H. E. Türeci, Cavity-coupled double-quantum dot at finite bias: Analogy with lasers and beyond, *Phys. Rev. B* **90**, 125402 (2014).
- [30] Y.-Y. Liu, J. Stehlik, C. Eichler, M. J. Gullans, J. M. Taylor, and J. R. Petta, Semiconductor double quantum dot micromaser, *Science* **347**, 285 (2015).
- [31] Y.-Y. Liu, J. Stehlik, C. Eichler, X. Mi, T. R. Hartke, M. J. Gullans, J. M. Taylor, and J. R. Petta, Threshold Dynamics of a Semiconductor Single Atom Maser, *Phys. Rev. Lett.* **119**, 097702 (2017).
- [32] Y.-Y. Liu, K. D. Petersson, J. Stehlik, J. M. Taylor, and J. R. Petta, Photon Emission from a Cavity-Coupled Double Quantum Dot, *Phys. Rev. Lett.* **113**, 036801 (2014).

- [33] M. J. Gullans, Y.-Y. Liu, J. Stehlik, J. R. Petta, and J. M. Taylor, Phonon-Assisted Gain in a Semiconductor Double Quantum Dot Maser, *Phys. Rev. Lett.* **114**, 196802 (2015).
- [34] For single atom lasers there is, strictly speaking, no sharp threshold: the average photon occupation of the cavity \bar{n} increases continuously with increasing coupling strength λ (see Ref. [43]). However, there is a smooth crossover occurring around a typical value of the coupling constant λ_c between one region in which the phonon occupation is practically zero and a second region in which the cavity starts to be occupied. Eventually, the phonon occupation saturates by further increasing λ . The semiclassical method, which predicts a sharp critical transition, yields an accurate estimate for λ_c (see Ref. [39]).
- [35] A. V. Rozhkov and D. P. Arovas, Interacting-impurity Josephson junction: Variational wave functions and slave-boson mean-field theory, *Phys. Rev. B* **62**, 6687 (2000).
- [36] Notice that the regime here discussed is different from the lasing regime discussed in Ref. [33] in which the longitudinal interaction of the double dot with both the cavity photons and the environment phonons leads to the simultaneous emissions of a phonon and a photon. This is crucial to achieve the phonon-assisted gain realized in the experiments of Refs. [30,31].
- [37] S. Braig and K. Flensberg, Vibrational sidebands and dissipative tunneling in molecular transistors, *Phys. Rev. B* **68**, 205324 (2003).
- [38] J. Koch, M. Semmelhack, F. von Oppen, and A. Nitzan, Current-induced nonequilibrium vibrations in single-molecule devices, *Phys. Rev. B* **73**, 155306 (2006).
- [39] M. Scully and M. Zubairy, *Quantum Optics* (Cambridge University Press, Cambridge, 1997).
- [40] M. G. Pala, M. Governale, and J. König, Nonequilibrium Josephson and Andreev current through interacting quantum dots, *New J. Phys.* **9**, 278 (2007).
- [41] M. Governale, M. G. Pala, and J. König, Real-time diagrammatic approach to transport through interacting quantum dots with normal and superconducting leads, *Phys. Rev. B* **77**, 134513 (2008).
- [42] A. Braggio, M. Governale, M. G. Pala, and J. König, Superconducting proximity effect in interacting quantum dots revealed by shot noise, *Solid State Commun.* **151**, 155 (2011).
- [43] Y. Mu and C. M. Savage, One-atom lasers, *Phys. Rev. A* **46**, 5944 (1992).
- [44] J. Gramich, A. Baumgartner, and C. Schönenberger, Resonant and Inelastic Andreev Tunneling Observed on a Carbon Nanotube Quantum Dot, *Phys. Rev. Lett.* **115**, 216801 (2015).